

# State Discretization for Continuous-State MDPs in Infectious Disease Control

Suyanpeng Zhang <sup>a</sup> and Sze-chuan Suen <sup>a</sup>

<sup>a</sup>Daniel J. Epstein Department of Industrial and Systems Engineering, Viterbi School of Engineering, University of Southern California, Los Angeles, CA, USA

## ARTICLE HISTORY

Compiled April 22, 2024

## ABSTRACT

Repeated decision-making problems under uncertainty may arise in the health policy context, such as infectious disease control for COVID-19 and other epidemics. These problems may sometimes be effectively solved using Markov decision processes (MDPs). However, the continuous or large state space of such problems for capturing infectious disease prevalence renders it difficult to implement tractable MDPs to identify the optimal disease control policy over time. We therefore develop an algorithm for discretizing continuous states for approximate MDP solutions in this context. We benchmark performance against a uniform discretization using both a synthetic example and an example of COVID-19 in Los Angeles County.

## KEYWORDS

State discretization; Markov decision processes; Infectious disease control; COVID-19; Continuous state

## 1. Introduction

Public health officials often need to determine the optimal health intervention policy over time while facing substantial uncertainty about the state and trajectory of disease in a population. Many of these problems require making policy decisions sequentially over time, where the state may be represented using a continuous measure (e.g., the proportion of the population that is infected). For instance, during the COVID-19 pandemic, decision-makers needed to repeatedly set the start and end times of lockdowns that limited travel and interactions between individuals to reduce transmission without fully understanding the exact transmissibility of COVID-19. This sequential decision-making problem under uncertainty appears repeatedly in infectious disease control, as evidenced by prior literature on similar problems (Blower, Koelle, & Mills, 2002; Fu, Jin, Xiang, & Wang, 2022; Kaplan, Anderson, et al., 1996; Matrajt et al., 2021; Talbot et al., 2005; F. Zhang, Wagner, & Ross-Degnan, 2011). Such problems often take into account underlying disease dynamics, which are uncertain or depend on a variety of complex social and biological factors.

A difficulty in solving repeated decision making problems for infectious disease control is the complexity of infectious disease dynamics, which are typically represented using compartmental models and simulation-based models (Brauer, 2008; Kopec et al.,

2010). Such models are difficult to use for repeated decision-making problems as one often needs to evaluate the model repeatedly to identify an optimal policy for disease control, which may require a significant investment of computational time, as there is no closed-form solution.

While there are sophisticated means to identify optimal policies, these techniques have their own challenges. For instance, the maximum principal approach (Goenka, Liu, & Nguyen, 2014; Piguillem & Shi, 2022; Pontryagin, 2018) offers a solution framework for optimal control issues under differential equation systems. However, its application becomes increasingly challenging with a large number of states or policies. Such expansion complicates both the Hamiltonian and the differential equations system, thereby rendering the process of deriving analytical or numerical solutions complicated and time-consuming. Moreover, it is difficult to find the optimal solution when the problem is non-convex. Simulation optimization, which can handle complex systems, has also been used in disease contexts (Carson & Maria, 1997). However, this can also be computationally expensive and time-consuming. Furthermore, the quality of the solution highly depends on the search space and the heuristic function chosen, presenting challenges to its practical application. One can formulate the infectious disease problem as a dynamic programming (Calvia, Gozzi, Lippi, & Zanco, 2023) problem, but the continuous or large state space can create difficulties.

Dynamic programming methods such as Markov decision processes (MDPs), are also a commonly used method for repeated decision making under uncertainty. MDPs allow for uncertainty in state transitions, which can be used to describe changes in disease/health states over time and allow for repeated decisions over time. Given current computing innovations, many MDPs of useful size can be solved effectively using algorithms such as backward induction, value iteration, policy iteration, etc. MDPs can also be efficiently solved with non-convex problems. Additionally, they inherently account for uncertainty in the outcomes of actions through transition probabilities.

However, incorporating dynamics from compartmental models and simulations into an MDP framework is challenging because disease models often use a continuous or large number of possible states (as the state usually represents a proportion of the whole population in certain statuses like infected, recovered, and hospitalized). Having a continuous state space makes the MDP problem difficult to solve since traditional MDP solution methods may then not work even for a short time horizon due to state-space explosion issues. For example, backward induction need  $|S|^2|A||T - 1|$  multiplications. In the case of value iteration, each iteration carries a complexity of  $\mathcal{O}(|S|^2|A|)$ . In the case of policy iteration, each iteration carries a complexity of  $\mathcal{O}(|S|^3 + |S|^2|A|)$ , and modified policy iteration requires  $\mathcal{O}(k|S|^2 + |S|^2|A|)$  per iteration (Puterman, 1994). For this reason, many traditional MDP studies in the healthcare field focus on finite-state decision-making problems like monitoring, treatment initiation, and disease testing and diagnosis (Ahn & Hornberger, 1996; Alagoz, Chhatwal, & Burnside, 2013; Alagoz, Maillart, Schaefer, & Roberts, 2004, 2007; Capan, Ivy, Wilson, & Huddleston, 2017; Chhatwal, Alagoz, & Burnside, 2010; David & Yechiali, 1985; Denton, Kurt, Shah, Bryant, & Smith, 2009; Hu, Lovejoy, & Shafer, 1996; Kreke, 2007; Kurt, Denton, Schaefer, Shah, & Smith, 2011; Lefèvre, 1981; Liu, Brandeau, & Goldhaber-Fiebert, 2017; Magni, Quaglini, Marchetti, & Barosi, 2000; Maillart, Ivy, Ransom, & Diehl, 2008; Mason, Denton, Shah, & Smith, 2014; Shechter, Bailey, Schaefer, & Roberts, 2008; Suen, Brandeau, & Goldhaber-Fiebert, 2018; S. Zhang et al., 2021). Therefore, finding a good state discretization method that translates infectious disease dynamics onto a limited number of states improve computational efficiency and potentially

widen the scope of MDP applications, particularly in the infectious disease space.

Uniform discretization is a traditional way of addressing continuous state problems. However, this methodology is suboptimal for addressing infectious disease control challenges. The heterogeneity in state visit frequencies—wherein some states (with extremely high prevalence) may remain unvisited and others (with lower prevalence) might be visited more frequently—renders uniform discretization inefficient. This approach may result in the overuse of discretizations towards states that are less likely to be visited and an inadequate number of discretizations for those with higher probabilities of being reached. How can we find a better way of discretizing the state space to closely represent the changes in health systems/disease? While many works have used various discretization methods to reduce state spaces (Lovejoy, 1991; Sandıkçı, Maillart, Schaefer, & Roberts, 2013), we take a novel approach that treats the state discretization problem as an optimization problem. This allows us to find the discretization that will provide a smaller discretized region in more likely visited states for a more accurate description of the true dynamics.

We will explore the above state discretization in the context of a disease control problem where states are used to describe the disease dynamics over a population, actions are implemented to prevent disease spread (lockdown, social distancing, face masks, and so on). States are assumed to be fully observable at each time period. Under this framework, we find a better way of discretizing states such that the discretized state space serves as a good proxy of the original state space. This paper addresses the challenge of formulating infectious disease control problems as MDPs by proposing a new algorithm for non-uniform state discretization that enables the discrete representation of infinite state spaces.

### ***1.1. Contributions***

We make several contributions in this study. We provide a novel algorithm for defining a non-uniform, discrete state space for infectious disease control problems that well approximates the original continuous state dynamics. Our algorithm exploits the likelihood of each state being visited in the system to more efficiently capture the transitions between states. Defining a discrete set of states from an originally continuous system allows us to incorporate infectious disease dynamics within frameworks that are better suited for discrete state spaces, such as MDPs. Finally, we demonstrate that our state space discretization allows for more accurate MDP outcomes through two numerical examples, one using a classic SIR compartmental model and one using COVID-19 model of Los Angeles County.

The remainder of this paper is organized as follows: we review the related literature in Section 2, present the problem setup in Section 3, and provide the algorithms in Section 4. The numerical example is shown in Section 5. In Section 6, we conclude.

## **2. Literature Review**

### ***2.1. Markov Decision Processes in Healthcare Applications***

MDPs have a rich history in the field of operations research, with wide range of applications such as inventory management (Giannoccaro & Pontrandolfo, 2002), portfolio management (Bäuerle & Rieder, 2009), production and storage optimization (Arruda & do Val, 2008), and various others. Extensive research has been conducted

to solve and understand the structure of MDPs, with notable contributions from works such as (Puterman, 1994) and (Topkis, 2011).

MDPs also find widespread application in the field of healthcare. They offer valuable insights and solutions to various health-related issues, including screening (Alagoz et al., 2013; Chhatwal et al., 2010; Maillart et al., 2008), sequential disease testing (Arruda, Pereira, Thiers, & Tura, 2019; Singh, Liu, & Shroff, 2020), treatment initiation (Liu et al., 2017; Shechter et al., 2008), and organ transplantation (Sandıkçı, Maillart, Schaefer, Alagoz, & Roberts, 2008; Sandıkçı et al., 2013; S. Zhang et al., 2021). For instance, patients in different age groups with risks of breast cancer may need personalized mammography exam frequencies (Alagoz et al., 2013), or, in another example, a patient with organ failure may be presented at different states with organ transplant options that vary in their compatibility with the patient. The patient may face the decision to either wait for a better match or accept an offered organ as their own survival probability decreases over time (S. Zhang et al., 2021). For a more extensive exploration of MDPs in healthcare, refer to the comprehensive reviews by Schaefer, Bailey, Shechter, and Roberts (2004), Alagoz, Hsu, Schaefer, and Roberts (2010), and Sonnenberg and Beck (1993). Although MDPs are widely used in healthcare applications, most of these consider finite-state decision-making. Constructing an MDP for infectious disease control problems with repeated decisions is challenging, especially when the state space for such problems is continuous.

## ***2.2. Solving Continuous State MDP***

As previously discussed, an infinite or continuous state space is a major challenge when formulating MDPs. Several methods have been proposed to address this problem. In Munos and Moore (2002), different criteria for discretizing state and time space non-uniformly are discussed. These methods involve evaluating values or policies using dynamic programming; however, some of these methods raise computational concerns for problems with continuous or large numbers of states. Brooks, Makarenko, Williams, and Durrant-Whyte (2006) proposed a parametric method to discretize a continuous state space by constraining distributions over state space to a parametric family. However, since prior knowledge of the distribution is required, MDPs for population-level infectious disease control would be difficult to solve in this manner. One remedy is to solve the MDP formulation by truncation and discretization of the state (Boucherie & Van Dijk, 2017). Researchers have used various methods to achieve this. For example, Zhou, Fu, and Marcus (2010) used Monte-Carlo simulation to approximate the belief state by a finite number of particles on a discretized grid mesh. Sandıkçı et al. (2013) used fixed-resolution, non-uniform grids to discretize the belief state and approximate the optimal policy for a partially observable MDP (POMDP) model. Lovejoy (1991) used fixed or uniform grids to approximate the solution of the POMDP. However, using uniform or pre-defined discretizations (which requires domain knowledge) may not always be appropriate, particularly for infectious disease control problems where disease spread is subject to uncertainty across different policy scenarios. In such cases, a more effective discretization algorithm is needed to enable the computation of the optimal policy.

### 2.3. Modeling Disease Dynamics

To identify the optimal policy for an infectious disease control problem, it is necessary to have a model for describing the disease dynamics. For instance, during an emerging pandemic, how would disease transmission change if the government imposed a 1-month lockdown? How would it change if the government imposed a 3-month lockdown instead? Different policies may change the patterns of disease transmission and thus change the proportion of infections in total. To efficiently avert infections, these different possibilities need to be evaluated to understand the resultant health and cost outcomes. Multiple methods are available for assessing the impact of different policies on a specific population.

One common method to model disease dynamics is to use compartmental models based on differential equations (Brauer, 2008; W. Kermack & McKendrick, 1991; W. O. Kermack & McKendrick, 1991a, 1991b). A compartmental model uses a mathematical framework to provide insights into the mechanism that affect the transmission and progression of disease. This framework partitions the population into different health or treatment states (compartments). For instance, each compartment represents a specific stage of the infectious disease (e.g., susceptible, infected, recovered), and proportions of the population move between compartments described by differential equations at certain rates. This model is fundamental in epidemiology for understanding the spread of diseases and evaluating the potential impact of public health interventions. For example, compartmental models can compare the effectiveness of wearing masks and social distancing during the COVID-19 pandemic (Grimm, Mengel, & Schmidt, 2021; Kai, Goldstein, Morgunov, Nangalia, & Rotkirch, 2020). Long, Nohdurft, and Spinler (2018) use a classical compartmental model to assist with the decision of allocating resources during the 2014 Ebola outbreak in Africa. In Section 5, we consider a classic Susceptible-Infected-Recovered (SIR) epidemic model, which has been extensively used in the epidemiological literature (Beckley et al., 2013; Harko, Lobo, & Mak, 2014; Kröger & Schlickeiser, 2020).

Another method of evaluating disease dynamics is to use simulation models, which can be used to track transmission, progression, and behavior as well as policy outcomes. For instance, simulation models can be employed to examine the cost-effectiveness of screening recommendations for positive-HIV men who have sex with men (MSM) (Tuite, Burchell, & Fisman, 2014), as well as to study the effectiveness of different disease control strategies for tuberculosis (TB) in India (Suen, Bendavid, & Goldhaber-Fiebert, 2014). Although these methods indeed capture the dynamics of complicated diseases, they are unable to compute dynamic policies effectively as  $m^t$  evaluations are usually needed when there are  $m$  possible interventions and  $t$  decision epochs. Therefore, it is beneficial to find alternative effective ways of identifying the optimal policy for infectious disease control. In our paper, we consider a discrete-state MDP framework that takes advantage of its effective solution methods with underlying disease dynamics estimated from traditional disease models such as compartmental and simulation models.

To model this problem as a discrete-state MDP, we also need to define a transition function to describe the probability of transitioning between the states. Several existing techniques can be used to construct this function. For instance, Yaesoubi and Cohen (2011) proposed a way to compute transition probabilities given a system of ODEs. In another example, Mishalani and Madanat (2002) proposed a method of developing transition probabilities from a stochastic duration model based on the hazard rate function. However, these methods are computationally intensive, which limits their

usage to problems with small populations or disease models with special structures.

### 3. Problem Setup

The notation used in this paper is as follows. We denote  $\mathbf{X}_t \in \mathcal{X}$  as the state of the epidemic at time  $t$ .  $\mathbf{X}_t = [X_{1t}, X_{2t}, \dots, X_{nt}]$  has  $n$  components where each represents the proportion of the population in the compartment (e.g., for a SIR model,  $n = 3$ ). For example,  $\mathbf{X}_t = [X_{St}, X_{It}, X_{Rt}] \in [0, 1]^3$  can describe the proportion of the population in susceptible (S), infected (I), and recovered (R) compartments at time  $t$  for a SIR model. We denote  $\mathbf{X}_0$  as the initial state and we assume it follows an initial distribution  $\Omega$ . We use  $\{\mathbf{X}_t\} = (\mathbf{X}_0, \dots, \mathbf{X}_N)$  to denote the disease trajectory.

In this paper, we focus on the finite horizon problem. Let  $T = \{1, \dots, N\}$  be the set of possible decision epochs for the problem.  $A = \{1, \dots, |A|\}$  is the set of possible policy interventions for the problem. We assume a small, finite number of actions/policies (e.g., lockdown versus no lockdown). We denote  $\pi_t \in A$  as the policy intervention at time  $t$ .

We consider a model denoted by  $f(\mathbf{X}_t, \pi_t) = \mathbf{X}_{t+1}$  that describes the disease dynamics across time epochs  $t$ . This function  $f(\mathbf{X}_t, \pi_t)$  can consider disease progression, transmission over time, mortality, and interventions. Generally,  $f(\mathbf{X}_t, \pi_t)$  takes the state of the system and policy intervention as an input and then returns the state in the next period. We assume that  $f(\mathbf{X}_t, \pi_t)$  is time-homogeneous for simplicity (if time-inhomogeneous dynamics are desired, our methods can be easily extended).

The cost in state  $\mathbf{X}_t \in \mathcal{X}$  and taking action  $\pi_t \in A$  for  $t \in T$  in the infectious disease control problem is denoted using  $r(\mathbf{X}_t, \pi_t)$ . This cost can be dependent on health outcomes (e.g., number of infected, total vaccinated population, etc.) as well as other factors (financial cost, economic burden, etc.). We let  $\lambda$  denote the discount factor.

Given the transition function  $f(\mathbf{X}_t, \pi_t)$  and the cost function  $r(\mathbf{X}_t, \pi_t)$ , we have the following optimization formulation for our repeated decision-making disease control problem:

$$\min_{\pi_0, \dots, \pi_{N-1}} \sum_t^N \lambda^t r(\mathbf{X}_t, \pi_t) | \mathbf{X}_0 \quad (1)$$

$$s.t. \quad \mathbf{X}_t = f(\mathbf{X}_{t-1}, \pi_{t-1}) \quad (2)$$

In the above problem, the objective is to find a sequence of actions  $\{\pi_0, \dots, \pi_{N-1}\}$  that minimizes the total discounted cost function  $r(\mathbf{X}_t, \pi_t)$  over states  $\mathbf{X}_t$  for the whole  $N$ -period time horizon given a known initial state  $\mathbf{X}_0$ . For example,  $\mathbf{X}_t$  can represent the proportion of individuals in each COVID-19-related health stage at time  $t$ , and let  $r(\mathbf{X}_t, \pi_t)$  compute the proportion of people dead from COVID-19 at time  $t$ . If  $\pi_t$  denotes the policy intervention (lockdown or not) at time  $t$ , then  $f(\mathbf{X}_{t-1}, \pi_{t-1})$  could be a system of difference equations that describes the population flow across different health stages. Our objective in this problem then is to find the optimal policy intervention at each time  $t$  that minimizes the total cost within  $N$  periods.

There are challenges to solving the above formulation using traditional MDP solution methods (e.g., backward induction, value iteration, policy iteration, etc.) as this formulation usually contains constraints with non-linear dynamics on a continuous state space. These solution methods require a finite number of states for effec-

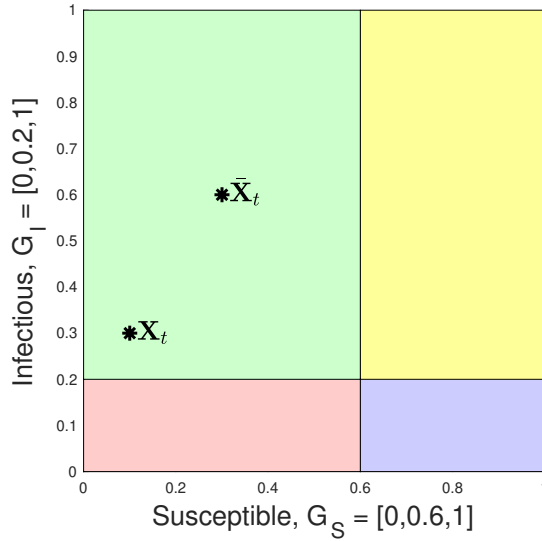


Figure 1.: Four regions defined using  $G = \{[0, 0.6, 1], [0, 0.2, 1]\}$  are shown in different colors. These correspond to four states: (1) :  $[\bar{X}_S, \bar{X}_I] = [0.3, 0.1]$ ; (2) :  $[\bar{X}_S, \bar{X}_I] = [0.3, 0.6]$ ; (3) :  $[\bar{X}_S, \bar{X}_I] = [0.8, 0.1]$ ; (4) :  $[\bar{X}_S, \bar{X}_I] = [0.8, 0.6]$ . For example,  $\mathbf{X}_t = [0.1, 0.3]$ , the corresponding discretized state representation is  $\bar{\mathbf{X}}_t = [0.3, 0.6]$ .

tive evaluation. Moreover, the function  $f(\mathbf{X}_t, \pi_t)$  may not be expressed as transition probabilities from state to state, while many traditional MDP solution methods use transition probability matrices to allow for the modeling of uncertainty and variability in decision-making processes.

To discretize the continuous state space, we partition the state space  $\mathcal{X}$  into a discrete set of states  $\mathcal{X}$ . For each component  $i$  in  $\mathcal{X}$ , we use the discretization vector  $G_i$  to describe how the continuous state space is partitioned into discrete states. The discretization vector  $G_i$  contains the maximal and minimal values of the discretized regions for component  $i$ . We use  $G$  to represent the list of discretization vectors for all components in  $\mathcal{X}$ . For instance, for an SI model, if  $G = \{[0, 0.6, 1], [0, 0.2, 1]\}$ , we mean that group 1 (the susceptible proportion of the population) is partitioned into two regions  $[0, 0.6)$  and  $[0.6, 1]$ , and the second group (infected proportion) is being partitioned into two regions  $[0, 0.2)$  and  $[0.2, 1]$ . In this case, we have a total of  $2 \times 2 = 4$  regions. These four regions are given by (1) :  $X_S \in [0, 0.6), X_I \in [0, 0.2)$ ; (2) :  $X_S \in [0, 0.6), X_I \in [0.2, 1]$ ; (3) :  $X_S \in [0.6, 1], X_I \in [0, 0.2)$ ; (4) :  $X_S \in [0.6, 1], X_I \in [0.2, 1]$  (shown in Figure 1).

From these regions, we capture the discretized state space in matrix  $\bar{\mathcal{X}}$ , which is comprised of the Euclidean centroids of each region. The dimension of  $\bar{\mathcal{X}}$  is  $|G| \times n$  where  $|G|$  is the number of regions and  $n$  is the number of components. Thus, in the example above, we would have four states. (1) :  $[\bar{X}_S, \bar{X}_I] = [0.3, 0.1]$ ; (2) :  $[\bar{X}_S, \bar{X}_I] = [0.3, 0.6]$ ; (3) :  $[\bar{X}_S, \bar{X}_I] = [0.8, 0.1]$ ; (4) :  $[\bar{X}_S, \bar{X}_I] = [0.8, 0.6]$ . In this case,

$$\bar{\mathcal{X}} = \begin{bmatrix} 0.3 & 0.1 \\ 0.3 & 0.6 \\ 0.8 & 0.1 \\ 0.8 & 0.6 \end{bmatrix}. \text{ Similarly, we define } \bar{\mathbf{X}}_t \in \bar{\mathcal{X}} \text{ to be the discretized state at time } t \text{ and}$$

$\{\bar{\mathbf{X}}_t\} = (\bar{\mathbf{X}}_0, \dots, \bar{\mathbf{X}}_N)$  to be the trajectory for the discretized state.

With this new discretized state space, we can now define  $\bar{f}(\bar{\mathbf{X}}_t, \pi_t, G)$ , the disease dynamics on the discretized state space. Even though the true disease dynamics might

be non-linear, we approximate the transitions on the discretized state space using a linear transition matrix. This is a reasonably good approximation if the length of  $t$  is sufficiently small.

We denote this transition probability matrix as  $P(\pi_t)$  for  $\pi_t \in A$ .  $P(\pi_t)$  has the dimension of  $|\bar{\mathcal{X}}| \times |\bar{\mathcal{X}}|$  where  $|\bar{\mathcal{X}}|$  is the size of the state space. Then the probability of the system being in a state at time  $t + 1$ ,  $\bar{\mathbf{X}}_{t+1}$ , given it was in state  $\bar{\mathbf{X}}_t$  at time  $t$  and policy intervention  $\pi_t \in A$  is denoted as  $P(\bar{\mathbf{X}}_{t+1}|\bar{\mathbf{X}}_t, \pi_t)$ .

Let  $V_t(\bar{\mathbf{X}}_t)$  denote the optimal value function of the discretized state  $\bar{\mathbf{X}}_t \in \bar{\mathcal{X}}$ ,  $t \in T$  for the discretized infectious disease control problem. At optimality, the following must hold:

$$V_t(\bar{\mathbf{X}}_t) = \max_{\pi_t \in A} \left\{ r(\bar{\mathbf{X}}_t, \pi_t) + \lambda \sum_{\bar{\mathbf{X}}_{t+1} \in \bar{\mathcal{X}}} P(\bar{\mathbf{X}}_{t+1}|\bar{\mathbf{X}}_t, \pi_t) V_t(\bar{\mathbf{X}}_{t+1}) \right\}$$

### 3.1. State Space Discretization Problem

With the original system  $f(\mathbf{X}_t, \pi_t)$  and state space  $\mathcal{X}$ , we aim to find the discretized state space  $\bar{\mathcal{X}}$  and the transition matrices  $P$  that approximate well the original system in that it gives a similar objective value  $V_t(\bar{\mathbf{X}}_t)$ , trajectories  $\{\bar{\mathbf{X}}_t\}$  given  $\{\pi_0, \dots, \pi_{N-1}\}$ , and a small optimality gap. In order to do this, we need to find a suitable  $G$  and map from  $\bar{f}(\bar{\mathbf{X}}_t, \pi_t, G)$  to  $P$ .

We focus on approximating the original system by establishing an appropriate discretization approach. An effective discretization method should consist of a small number of discretized states that consider intervention effects. To do this efficiently, the discretized states should be capable of providing higher precision in areas where the state space is more likely to be visited. This can lead to a better approximation of the true disease dynamics and can thus result in a more accurate MDP solution.

Given the function  $f(\mathbf{X}_t, \pi_t)$ , the initial state, the time horizon, and a sequence of policies  $\{\pi_0, \dots, \pi_{N-1}\}$ , we can calculate a trajectory  $\{\mathbf{X}_t\}$ . Subsequently, we require a state discretization  $G$  that ensures the discretized trajectory  $\{\bar{\mathbf{X}}_t\}$  closely approximates  $\{\mathbf{X}_t\}$  for various initial states and policies. Therefore, our objective is to minimize the distance between the true trajectory and trajectory from the discretized model over all samples  $\theta = (\mathbf{X}_0, \{\pi_0, \dots, \pi_{N-1}\}) \in \Theta$ , all policy intervention scenarios  $\pi_t$ , and all time, i.e., minimizing  $\sum_{\theta \in \Theta} \sum_{t=1}^N \|\mathbf{X}_t - \bar{\mathbf{X}}_t\|_2 \mid \theta$ . Given a sequence of policy intervention  $\{\pi_0, \dots, \pi_{N-1}\}$  and an initial state  $\mathbf{X}_0$ , we compute the true trajectory using  $f(\mathbf{X}_t, \pi_t)$ . We use  $\bar{f}(\bar{\mathbf{X}}_t, \pi_t, G)$  to compute the trajectory from the discretization space matrix  $\bar{\mathcal{X}}$ .

We then map the transition function for discretized states  $\bar{f}(\bar{\mathbf{X}}_t, \pi_t, G)$  to transition probability matrix  $P$ . Various existing techniques help to construct transition probabilities given function  $\bar{f}(\bar{\mathbf{X}}_t, \pi_t, G)$ . We discuss how to find a generalizable and efficient way of computing transition probabilities from  $\bar{f}(\bar{\mathbf{X}}_t, \pi_t, G)$  given the state discretization in the next section.

## 4. Algorithms

In this section, we present a generalizable framework for discretizing a continuous state space for use in MDP frameworks and correspondingly constructing transition probability matrices.



#### 4.1. Greedy Algorithm for Finding Discretizations (GreedyCut)

The main objective of discretization is to design an effective approach for approximating the disease dynamics with a high level of accuracy, making such problems tractable for conventional discrete-space MDP frameworks. However, it would not be advantageous if the process of finding discretizations itself becomes excessively costly. Therefore, our motivation is to identify a low-cost method that can produce discretizations capable of representing the disease dynamics effectively. In particular, we are interested in outperforming a uniform discretization, which can be considered a general default discretization appropriate across many domains.

We assume there is a budget  $B$  that represents the total number of regions/discretizations we can have in realize of computational considerations. We use simulated initial states and policy interventions  $\theta = (\mathbf{X}_0, \{\pi_0, \dots, \pi_{N-1}\}) \in \Theta$  to find the discretizations.

The greedy approach has been widely applied to various optimization tasks, which is easy to implement and effective at finding solutions (Blanchard, Cermak, Hanle, & Jing, 2014; Wu, Luo, Xiong, Zhang, & Kim, 2018; Zhao, Zhou, & Liu, 2021). We now propose Algorithm 1 (GreedyCut), a greedy-based iterative approach to finding a good discretization.

In Algorithm 1, we have three functions. The cost function computes the sum of squared error between the trajectory from the discretized state space  $\{\bar{\mathbf{X}}_t\}$  and true trajectory  $\{\mathbf{X}_t\}$  from  $f(X_t, \pi_t)$ . We compute the discretized trajectory  $\{\bar{\mathbf{X}}_t\}$  using  $\bar{f}(\bar{\mathbf{X}}_t, \pi_t, G)$ , where the  $i$ -th component  $\bar{X}_{it} = \sum_{j=0}^{|G_i|-1} \mathbf{1}_{G_{i,j} \leq f(\bar{\mathbf{X}}_{t-1}, \pi_{t-1})_i < G_{i,j+1}} \frac{G_{i,j} + G_{i,j+1}}{2}$  takes the average value of the region it belongs to after the discretization. The cost function can also be customized (e.g., introduce another penalty term to emphasize certain disease compartments).

The cut function halves the  $i$ -th region of the  $d$ -th component to make two discretized regions from one continuous range. For example, if we apply  $CUT(1, 1, G)$  where  $G = \{[0, 0.6, 1], [0, 0.2, 1]\}$  is defined the same as Figure 1, then the new discretization  $G'$  becomes  $G' = \{[0, 0.3, 0.6, 1], [0, 0.2, 1]\}$ . The new discretization  $G'$  is shown in Figure 2b. After the cut, there are now 6 discretized regions.

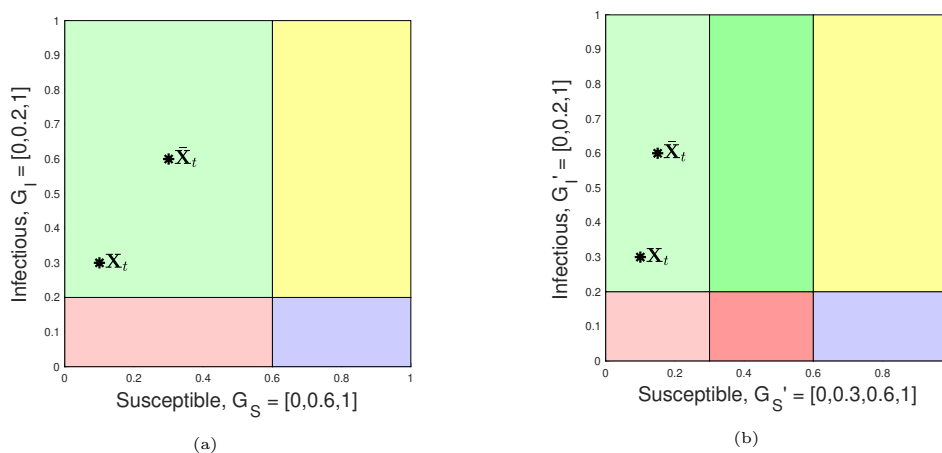


Figure 2.: Apply  $Cut(1,1,G)$  where  $G = \{[0, 0.6, 1], [0, 0.2, 1]\}$  gives new discretizations  $G' = \{[0, 0.3, 0.6, 1], [0, 0.2, 1]\}$ . In the new discretization, the  $\bar{\mathbf{X}}_t$  is changed as the Euclidean centroid where  $\mathbf{X}_t$  belongs to has changed. For  $G$ ,  $\|\mathbf{X}_t - \bar{\mathbf{X}}_t\|^2 = 0.11$ . For  $G'$ ,  $\|\mathbf{X}_t - \bar{\mathbf{X}}_t\|^2 = 0.0925$ .

The greedy function then iteratively computes the cost of cutting one continuous

---

**Algorithm 1** Iterative Discretization for Disease Control Problems
 

---

```

1: procedure COST( $\{\mathbf{X}_t\}, \{\bar{\mathbf{X}}_t\}$ )           ▷  $\{\mathbf{X}_t\}$  is the true trajectory,  $\{\bar{\mathbf{X}}_t\}$  is the
   trajectory from the discretization
2:   return  $\sum_{t=1}^N \|\bar{\mathbf{X}}_t - \mathbf{X}_t\|_2^2$ 
3: procedure CUT( $d, i, G$ )           ▷  $d$  is the component we want to cut, and we want to
   cut interval  $[i, i + 1]$  in half
4:    $G_d = [0, \dots, G_{d,i}, (G_{d,i} + G_{d,i+1})/2, G_{d,i+1}, \dots, 1]$ 
5:   return  $G$ 
6: procedure GREEDY( $B, G, f(\mathbf{X}_t, \pi_t), \bar{f}(\bar{\mathbf{X}}_t, \pi_t, G), \theta$ ) ▷  $B$  is the budget,  $f(\mathbf{X}_t, \pi_t)$ 
   is the compartmental model dynamics,  $\bar{f}(\bar{\mathbf{X}}_t, \pi_t, G)$  calculates the trajectory using
   discretized states  $\bar{\mathbf{X}}_t$ ,  $\Theta$  is the pre-generated samples of initial states and policies,
   for each  $\theta \in \Theta$ ,  $\theta = (\mathbf{X}_0, \{\pi_0, \dots, \pi_{N-1}\})$ 
7:   iter_per_sample =  $|\Theta|/B$ 
8:   for  $\theta \in \Theta$  do
9:     for iterations = 1 : iter_per_sample do
10:      best cost =  $UB$ 
11:      worst cost =  $LB$ 
12:      for Component  $d$  do
13:        for discretization  $i \in G_d$  do
14:          Compute  $\{\mathbf{X}_t\}$  using  $\mathbf{X}_t = f(\mathbf{X}_{t-1}, \pi_{t-1})$ 
15:          Compute  $\{\bar{\mathbf{X}}_t\}$  using  $\bar{\mathbf{X}}_t = \bar{f}(\bar{\mathbf{X}}_{t-1}, \pi_{t-1}, \text{Cut}(d, i, G))$ 
16:          tmp cost = Cost( $\{\mathbf{X}_t\}, \{\bar{\mathbf{X}}_t\}$ )
17:          if tmp cost < best cost then
18:            best cost = tmp cost
19:          if tmp cost > worst cost then
20:            worst cost = tmp cost
21:          if worst cost = best cost then
22:            draw a point  $X_{dt}$  from  $\{\mathbf{X}_t\}$ 
23:            update  $G = \text{Cut}(d, i, G)$  such that  $G_{d,i} \leq X_{dt} \leq G_{d,i+1}$ 
24:          else
25:            cut where cost is minimized
26:   return  $G$ 

```

---

range into two equal discretizations along each component (dimension) and finds the best cut. If each cut has the same cost, a point ( $X_{dt} \in \mathbf{X}_t$ ) from the sampled trajectory ( $\{\mathbf{X}_t\}|\theta$ ) will be randomly drawn, and the region that this point belongs to (component  $d$  of the region  $i$  of  $G$  such that  $G_{d,i} \leq X_{dt} \leq G_{d,i+1}$ ) will be cut into halves. When every cut incurs the same cost, we want to cut based on the data obtained through sampling. In general, it is unlikely that the costs for all cuts will be exactly the same; this might occur at the beginning of the algorithm when each discretized state encompasses a large range and the approximation will not improve if cut only once. Through this process, in total,  $|G| = \sum_d |G_d|$  discretizations will be generated.

#### 4.1.1. Complexity Analysis

In Algorithm 1, if we assume that computing  $\{\mathbf{X}_t\}$  and  $\{\bar{\mathbf{X}}_t\}$  using  $f(\mathbf{X}_t, \pi_t)$  and  $\bar{f}(\bar{\mathbf{X}}_t, \pi_t, G)$  requires  $K$  and  $\bar{K}$  operations respectively, we can analyze the total number of operations performed by the GreedyCut algorithm. Since the computational costs for generating new discretizations, comparing costs, and computing costs are relatively small compared to computing  $\{\mathbf{X}_t\}$  and  $\{\bar{\mathbf{X}}_t\}$  in our problem, we assume these costs are negligible compared with other costs. The GreedyCut algorithm enumerates through each discretization of  $b$  discretizations at the current iteration, where  $1 \leq b \leq |G|$ . For each discretization, the algorithm performs computations of  $\{\mathbf{X}_t\}$  and  $\{\bar{\mathbf{X}}_t\}$ , which have time complexities of  $K$  and  $\bar{K}$  operations respectively.

The total number of operations for the GreedyCut algorithm can be estimated as the sum of operations over all discretizations. This can be expressed as  $\sum_{b=1}^{|G|} b(K + \bar{K}) = \frac{|G|(|G|+1)}{2}(K + \bar{K})$ . Therefore, the complexity of the GreedyCut algorithm is on the order of  $\mathcal{O}(|G|^2(K + \bar{K}))$ . This implies that the complexity grows exponentially with the number of discretizations, given by  $|G|$ . The time complexity increases quadratically with  $|G|$  while linearly with the number of operations required for each discretization, represented by  $(K + \bar{K})$ .

As a result, the computational complexity of the algorithm grows rapidly as the number of discretizations increases. This highlights the exponential relationship between the complexity and the desired level of granularity in the discretization process.

## 4.2. Constructing a Corresponding Transition Matrix

Once a suitable discretization of a continuous state space has been constructed, we additionally need a transition matrix between these discretized states to capture the dynamics for use in an MDP framework. To do this, we present Algorithm 2, which draws samples from each discretized state to determine the frequency of transitions to subsequent states via the function  $f(\mathbf{X}_t, \pi_t)$  and  $G$ .

In Algorithm 2, we draw  $c$  samples within each region in  $G$  and count the frequency of the transitions from the current region to other regions using policy  $\pi_t$  and  $f(\mathbf{X}_t, \pi_t)$ . By sampling and counting the transitions from the original system, we approximate the underlying transition probabilities directly. Creating approximated transition probability matrices in this way offers a practical approach to capturing the essential dynamics of the system and enables efficient decision-making at the population level.

---

**Algorithm 2** Generating Transition matrix

---

```
1: procedure GENERATE( $f(\mathbf{X}_t, \pi_t), G$ ) $\triangleright$   $f(\mathbf{X}_t, \pi_t)$  is the ground-truth discrete time
   model,  $G$  is the discretization
2:   Let  $P$  be a  $|\mathcal{X}| \times |\mathcal{X}| \times |A|$  transition matrix with all zeros and each state
   represents a discretized state from the discretized state space  $\mathcal{X}$  defined by  $G$ 
3:   for each policy intervention  $\pi_t \in A$  do
4:     for each discretized state  $i$  from  $\mathcal{X}$  do
5:       Uniformly draw  $c$  number of samples ( $\hat{\mathbf{X}}_0$ ) within the region that con-
   tains  $i$  (including a centroid in this region)
6:       for each sample  $\hat{\mathbf{X}}_0$  do
7:         Compute  $\hat{\mathbf{X}}_1 = f(\hat{\mathbf{X}}_0, \pi_t)$ 
8:         Find the discretized state  $j$  such that the discretized region contains
    $j$  also contains  $\hat{\mathbf{X}}_1$ 
9:          $P(j|i, \pi_t) = P(j|i, \pi_t) + 1$ 
10:      Normalize  $P$  to make it a stochastic matrix
11:   return  $P$ 
```

---

#### 4.2.1. Complexity Analysis

In Algorithm 2, we generate  $c$  samples  $|G||A|$  times, where  $|G|$  denotes the number of discretizations and  $|A|$  represents the size of the action space. Assuming that computing and locating  $\hat{\mathbf{X}}_1$  in the appropriate discretization take  $\hat{K}$  operations, we can analyze the time complexity of Algorithm 2. The number of operations performed by the algorithm then is  $\mathcal{O}(c\hat{K}|G||A|)$ .

Furthermore, in most disease control problems, such as COVID-19 mitigation strategies like lockdown, social distancing, and face masks, the size of the action space  $|A|$  is typically small. This implies that the algorithm’s time complexity is primarily influenced by the number of samples  $c$ , the number of discretizations  $|G|$ , and the operations  $\hat{K}$  needed for computing and locating  $\hat{\mathbf{X}}_1$ .

## 5. Numerical Examples

In this section, we first showcase our proposed framework for reformulating a SIR model to an infectious disease control MDP framework for supporting public health decisions around social distancing policy. We then demonstrate the utility of this framework with an example of COVID-19 in Los Angeles County, drawing from empirical data of case counts in 2020.

We benchmark the outcome of our method (we refer to the ‘GreedyCut discretization method’ hereafter) in both examples by comparing our model outcomes to that of a uniform discretization framework. In this uniform discretization framework, we discretize the entire state space uniformly using the same number of discretizations as used in the GreedyCut discretization method. We then construct the transition probability matrix using Algorithm 2. The transition probabilities for both methods are generated using Algorithm 2. In the second example, we additionally compare our model outcomes to the empirical status-quo policy in Los Angeles in 2020 to demonstrate the improvement our method can achieve.

### 5.1. Example 1: A Simple SIR Model

The SIR model tracks the proportion of the population that is susceptible ( $S$ ), infected ( $I$ ), and recovered ( $R$ ) at each time  $t$ . We use a discrete time model where the SIR model can be described using a system of difference equations (Allen, 1994):

$$\begin{aligned} S_{t+1} &= S_t - \beta S_t I_t \\ I_{t+1} &= I_t + \beta S_t I_t - \gamma I_t \\ R_{t+1} &= R_t + \gamma I_t \end{aligned}$$

The parameter  $\beta$  is the rate at which disease transmits from the infected to susceptible population proportions, and is dependent on the average contact rate and probability of transmission given a discordant contact. Similarly,  $\gamma$  is the recovery rate.

Typically, at the beginning of an epidemic, the exact proportion of the population that is infected may be unknown. We use  $\mathbf{X}_0 = [X_{S0}, X_{I0}, X_{R0}] = [S_0, I_0, R_0]$  to denote the initial state at the first decision epoch. We assume that while the exact initial state is unknown, we know an upper and lower bound on each of the compartments. We use  $\underline{S}, \bar{S}, \underline{I}, \bar{I}$ , and  $\underline{R}, \bar{R}$  to denote the upper and lower bound on initial states  $S_0, I_0$ , and  $R_0$ , respectively.

Suppose at each time  $t$ , the health department can choose to implement a social distancing policy (a “lockdown”) until time epoch  $t + 1$  that reduces the transmission rate  $\beta$ . We assume there are a finite number of periods  $N$ .

The decision maker wishes to minimize the negative health outcomes and economic and social costs of implementing a lockdown policy. To capture this objective, at each decision epoch, we let the cost be  $r(\mathbf{X}_t, \pi_t) = I_t + u(\pi_t)$ , the proportion of the population infected ( $I_t$ ) plus some time-invariant dis-utility value  $u(\pi_t)$  that captures the economic and social costs that are only incurred when the intervention is in effect and zero otherwise.

Throughout this section, we refer to this discrete time system as the ground-truth system, and we will construct our discretized MDP framework based on this. We assume no discounting in the objective ( $\lambda=1$ ). The objective of the MDP is therefore to minimize the total costs over the whole time horizon.

#### 5.1.1. Inputs

To evaluate this example, we let the transmission rate ( $\beta$ ) be 1.4 and the recovery rate ( $\gamma$ ) be 0.49. The decision interval ( $\Delta t$ ) is a week, and the time horizon ( $N$ ) is ten weeks. Implementing a lockdown will incur an economic and social cost, but it is unclear how this dis-utility can be quantified in reality. For simplicity, we assume the dis-utility is 0.03 if lockdown was implemented and 0 otherwise ( $u(\text{lockdown}) = 0.03, u(\text{no lockdown}) = 0$ ).

During the early stages of a pandemic, there is typically a large population in the susceptible category, while only a small population is infected. Therefore, we choose the initial states to be uniformly distributed within the upper and lower bounds for each compartment to be:  $[\underline{S}, \bar{S}] = [0.7, 0.99]$ ,  $[\underline{I}, \bar{I}] = [0.01, 0.1]$ , and  $[\underline{R}, \bar{R}] = [0, 0.29]$ .

In the GreedyCut discretization method, for each sample ( $\theta$ ) generated, ten iterations are run to generate ten additional discretizations (lines 9 - 24 in Algorithm 2). To generate samples  $\theta$ ,  $\mathbf{X}_0$  are generated uniformly from the region above, and  $\pi$  is a vector with ten random binary variables to indicate the policy intervention (0 – no

lockdown,  $1 - \text{lockdown}$ ). In Algorithm 2, we generate  $c = 1000$  samples to compute two transition probability matrices to correspond to the no lockdown and lockdown policies, respectively.

### 5.1.2. MDP Solutions

We compare MDP solutions between the GreedyCut and the uniform discretization methods on 90, 150, 300, and 1200 discretizations.

To evaluate our algorithm’s performance, we create 300 samples (we denote the set of all samples as  $\tilde{\mathbf{X}}_0$ ) by selecting the initial susceptible proportion from 0.7 to 0.99 with stepsize of 0.01 and initialize the infected proportion from 0.001 to 0.01 with 0.001 stepsize. By enumerating each pair of  $S$  and  $I$ , we can have a total of 300 different possible initial states (if  $S + I > 1$ , we will renormalize each compartment). We compute the following metrics for both GreedyCut and uniform discretization methods on 90, 150, 300, and 1200 discretizations:

- ACC: accuracy in matching the percentage of optimal actions by comparing discretized MDP with brute force (ground-truth) solution over each state-time pair (a total of 3000 state-time pairs).  $\text{ACC} = 1 - \frac{\#mismatch}{3000}$ .
- MSE: mean squared error between the optimal value of the discretized MDP ( $\tilde{V}_0^*$ ) and the brute force solution ( $V_0^*$ ) on the first decision epoch over all states.  $\text{MSE} = \mathbb{E}_{\mathbf{X}_0 \in \tilde{\mathbf{X}}_0} [|\tilde{V}_0^*(\mathbf{X}_0) - V_0^*(\mathbf{X}_0)|^2]$ .
- E2: relative mean absolute error on the first decision epoch over all states.  $\text{E2} = \mathbb{E}_{\mathbf{X}_0 \in \tilde{\mathbf{X}}_0} \left[ \frac{|\tilde{V}_0^*(\mathbf{X}_0) - V_0^*(\mathbf{X}_0)|}{V_0^*(\mathbf{X}_0)} \right]$ .
- Opt. Gap: average of the relative difference between the optimal value of brute force solution and the value of running optimal policy from discretized MDP on the true disease model ( $\tilde{V}_0$ ) on the first decision epoch.  $\text{Opt. Gap} = \mathbb{E}_{\mathbf{X}_0 \in \tilde{\mathbf{X}}_0} \left[ \frac{|\tilde{V}_0(\mathbf{X}_0) - V_0^*(\mathbf{X}_0)|}{V_0^*(\mathbf{X}_0)} \right]$ .

The GreedyCut discretized MDP is able to generate solutions with a higher accuracy than the uniform discretized MDP. We compare the solutions from the GreedyCut and the uniform discretized MDPs against the brute force solution in the fifth week ( $t = 5$ ) for illustration. In the fifth week, we compare optimal actions across 300 states. The results indicate that the GreedyCut discretized MDP has six mismatches, whereas the uniform discretized MDP has 26 mismatches when compared with the brute force solution.

Moreover, the direction of error may be worse with the uniform discretization MDP. In the GreedyCut discretized MDP, all six mismatches belong to the case where the brute force solution recommends not to lockdown while the GreedyCut discretized MDP recommends implementing lockdown. However, in the uniform discretized MDP, all 27 mismatches belong to the case where the brute force solution recommends lockdown while the discretized MDP recommends not implementing lockdowns. In infectious disease control, failing to implement a lockdown when it is necessary can cause a rapid increase in the proportion of infected cases. Therefore, error in this direction may be practically worse than in the converse direction. We see this illustrated in the optimality gap between the two discretized MDPs (last columns in Table 1), which measures the distance between solutions from discretized MDPs and the true optimal solution. Here we see that GreedyCut MDP achieves a much lower optimality gap for this reason.

The GreedyCut discretization method outperforms the uniform discretization meth-

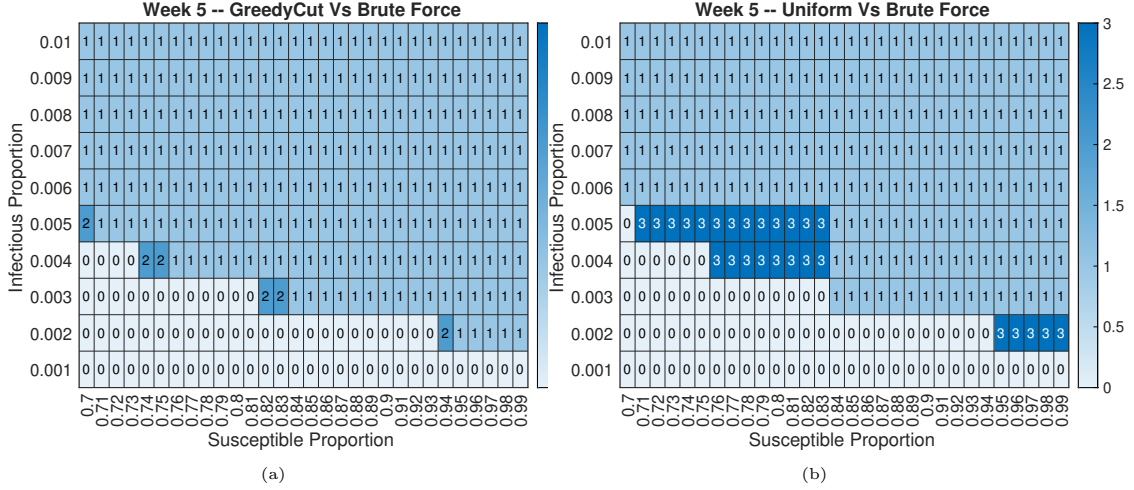


Figure 3.: We compare the optimal solution at  $t = 5$  across different states using the GreedyCut and uniform discretized MDPs against the ground truth optimal solution found using brute force methods. (a): Optimal solution from the GreedyCut discretized MDP compared to the brute force solution; (b): Optimal solution from the uniform discretized MDP compared to the brute force solution. ( 0 – both models recommend not implementing lockdown; 1 – both models recommend implementing lockdown; 2 – the brute force method recommends not implementing lockdown while the other method recommends lockdown [type 2 error]; 3 – the brute force method recommends implementing lockdown while the other method recommends not implementing lockdown [type 1 error].)

G	ACC		MSE		E2		Opt. Gap	
	GreedyCut	Uniform	GreedyCut	Uniform	GreedyCut	Uniform	GreedyCut	Uniform
90	0.9657	0.8120	4.3239e-04	0.0580	0.0689	0.8846	0.0033	0.0954
150	0.9850	0.8820	1.7896e-04	0.0169	0.0435	0.4946	0.0011	0.0583
300	0.9787	0.8613	6.5032e-05	0.0054	0.0233	0.2487	0.0018	0.0251
1200	0.9880	0.9150	3.1079e-05	4.3529e-04	0.0181	0.0654	0.0010	0.0072

Table 1.: Comparison on MDP solutions

ods across different evaluation metrics across all time periods and different discretization budgets. Table 1 shows the comparison between the GreedyCut and the uniform discretization methods. Also, the GreedyCut discretization method has higher accuracy (approximately 10% more) in matching the optimal actions from the brute force (ground-truth) solution over all state-time pairs. The GreedyCut discretization method is able to generate accurate recommendations on policy interventions even with a small number of discretizations. Additionally, this method is able to provide a closer approximation of the objective value in both MSE and E2 metrics across all discretizations. When the number of discretizations is small, the GreedyCut algorithm has an MSE that is under 1% of the MSE generated using the uniform discretization approach. Similarly, under these conditions, the GreedyCut algorithm’s E2 remains below 10% of the E2 from the uniform discretization method. Moreover, the GreedyCut algorithm outperforms the uniform discretization method in reducing the optimality gap. The optimality gap ranges from 0.1% to 0.33% with different numbers of discretizations in the GreedyCut algorithm, compared with its ranges from 0.72% to 9.54% in the uniform discretization method.

As expected, with a small number of discretizations, the difference in performance between the GreedyCut and the uniform discretization methods is large. The performance gap shrinks when the number of discretizations increases, as uniform discretizations naturally benefit from smaller discretized regions – higher resolution.

**Run Time Outcomes.** To understand how much time is needed to construct an MDP using the GreedyCut discretization method and Algorithm 2, we compare the run time of Algorithm 1 and Algorithm 2 with different numbers of discretizations using Matlab 2022b on a laptop with 16 GB memory and Apple M1 pro chip.

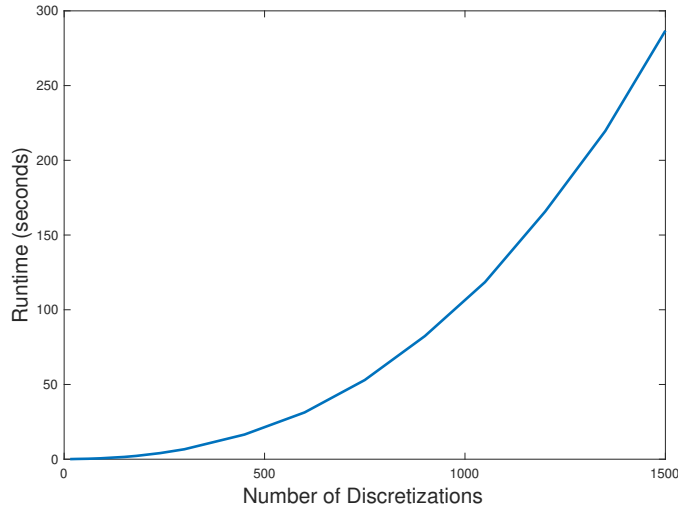


Figure 4.: Runtime of Algorithm 1

There is an exponential relationship between the number of discretizations and the algorithm runtime (see Figure 4), consistent with the time complexity analysis in Section 4.1.1. The curvature of the exponential function will depend on the complexity of the disease model  $f(\mathbf{X}_t, \pi_t)$ ; with more compartments or population stratifications, the total runtime may be larger for a similar number of discretizations.

$ G $	Runtime (hours):
90	0.12
150	0.34
>300	>1

Table 2.: Runtime of Algorithm 2

The runtime of generating transition matrices is much more costly compared with generating the discretizations when number of discretizations ( $|G|$ ) is small for both GreedyCut and uniform discretization. Table 2 shows the runtime of generating transitions using Algorithm 2 for the GreedyCut discretization method (the uniform discretization method should have the same runtimes as there are the same number of iterations needed). The runtime exceeds one hour with 300 discretizations given  $c = 1000$ . Therefore, when  $|G|$  is small, the total runtime of constructing an approximate MDP is roughly the time for generating transitions using Algorithm 2. In this case, the time that it takes to construct the MDP using the GreedyCut discretization method is close to that of using the uniform discretization method – because the runtime of the Algorithm 1 (which is only needed for GreedyCut and not the uniform discretization) is negligible compared to the runtime of Algorithm 2.



### 5.1.3. General Algorithm Evaluation

In this section, we evaluate the GreedyCut discretization method’s performance on generating discretizations that approximate the disease dynamics  $\{\mathbf{X}_t\}$  and Algorithm 2’s performance on generating transition probability matrices to generate the discretized trajectories  $\{\bar{\mathbf{X}}_t\}$ . We first examine the performance of Algorithm 2 to highlight its capability to generate precise transition probabilities. These probabilities are crucial for describing the discretized trajectory across various discretization settings. Subsequently, we assess the performance of the GreedyCut discretization method by comparing the Markovian trajectories (using transition probabilities from Algorithm 2) between the GreedyCut algorithm and uniform discretization method.

**How Accurate Are the Generated Transition Probabilities?** To evaluate the accuracy of generated transition probabilities from Algorithm 2, we draw samples and evaluate computed trajectories compared with trajectories  $\{\bar{\mathbf{X}}_t\}$  from  $\tilde{f}(\bar{\mathbf{X}}_t, \pi_t, G)$  to eliminate the influence of the quality of the discretization algorithm.

For evaluation, we uniformly draw 1000 samples ( $\hat{\theta} \in \hat{\Theta}$ ) that consist of initial states within the upper and lower bound of the proportions in each compartment and a sequence of policy interventions for each initial state. For each evaluation sample  $\hat{\theta}$ , we compute the discretized trajectory  $\{\bar{\mathbf{X}}_t\}$  using  $\tilde{f}(\bar{\mathbf{X}}_t, \pi_t, G)$ . To obtain the Markovian trajectories from the discretized Markov model, we use an initial belief  $b_0 = \mathbf{e}_i$  where all entries of  $b_0$  are zero except for  $i$ -th entry (corresponding to  $\mathbf{X}_0$ ) which has value one. This indicates we know 100% the initial state of the discretized Markov model. Then we update the belief  $b_t = P(\pi_t)b_{t-1}$  over time. To compute the expected proportion of people on each time  $t$  (Markovian trajectory at time  $t$ ,  $\tilde{\mathbf{X}}_t$ ), we use the weighted average over the belief vector at time  $t$ , e.g.,  $\tilde{\mathbf{X}}_t = b_t^T \bar{\mathcal{X}}$ . We then compute the cost  $\mathbb{E}_{\hat{\theta} \in \hat{\Theta}}[\sum_{t=1}^N \|\tilde{\mathbf{X}}_t - \bar{\mathbf{X}}_t\|_2^2]$  to evaluate how close is Algorithm 2 able to generate reliable transition probability matrices.

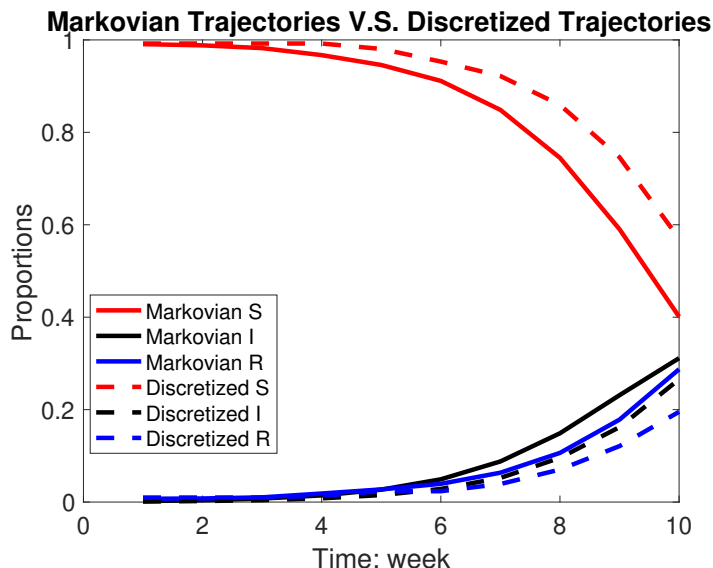


Figure 5.: Comparison between trajectories generated from Algorithm 2 given discretizations and trajectories generated from discretized states. For each compartment S, I, and R, both trajectories are close to each other.

The trajectories obtained from Algorithm 2 closely align with those generated from discretized states for each compartment. As shown in Figure 5, we compared the

trajectories obtained from Algorithm 2 using 300 discretizations with the  $\bar{f}(\bar{\mathbf{X}}_t, \pi_t, G)$  trajectories generated from the same 300 discretized states.

We observed that as the number of discretizations increases, Algorithm 2 is capable of generating transitions that closely resemble the dynamics of the disease, represented by  $\{\tilde{\mathbf{X}}_t\}$ . In Table 3, we show a comparison of the cost  $\mathbb{E}[\sum_{t=1}^N \|\tilde{\mathbf{X}}_t - \bar{\mathbf{X}}_t\|_2^2]$  for  $|G|$  of 90, 150, 300, and 1,200 using the GreedyCut discretization method. We observe that the population proportions generated using the Markovian and discretized processes closely align, even over time.

With fewer discretizations, each individual discretization possesses a larger range, making it more difficult for samples drawn from these discretizations to transition accurately between decision epochs, leading to more error in approximating  $\{\bar{\mathbf{X}}_t\}$ . On the other hand, when a larger number of discretizations is employed, each discretization exhibits a smaller range. By drawing a sufficient number of samples, it becomes possible to provide a more precise description of  $\{\tilde{\mathbf{X}}_t\}$ . These findings highlight the algorithm’s reliability and accuracy in capturing the system’s dynamics.

$ G $	Mean Squared Error Between Discretized Trajectory and Markovian Trajectory [95% uncertainty interval]	
90	0.4362	[0.3921, 0.4802]
150	0.1869	[0.1665, 0.2072]
300	0.1370	[0.1191, 0.1548]
1200	0.1212	[0.1075, 0.1349]

Table 3.: Mean squared error for the trajectories given different numbers of discretizations

**How Accurate Are the Discretizations Generated from the GreedyCut Discretization Method?** Next, to evaluate the quality of discretizations generated from the GreedyCut discretization method, we draw samples and calculate the mean squared error across all samples. This error is measured between the actual trajectory ( $\{\mathbf{X}_t\}$ ) and anticipated Markovian trajectory ( $\{\tilde{\mathbf{X}}_t\}$ ), using the transition matrix created in Algorithm 2 using the discretizations generated from Algorithm 1 based on the same 1000 samples for evaluating Algorithm 2.

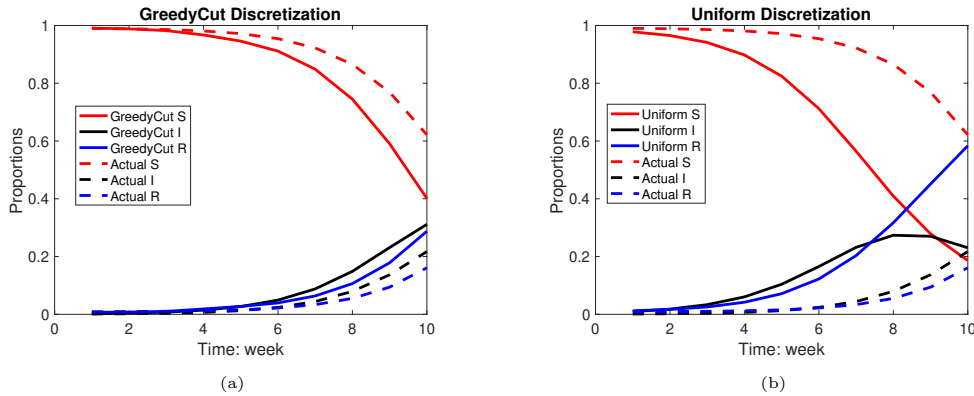


Figure 6.: Comparison between trajectories generated from the GreedyCut discretization method against the uniform discretization method (using 300 discretizations in total) given trajectories generated from SIR model. For each compartment S, I, and R, the GreedyCut discretization method can better capture the disease dynamics.

We use the same discretization levels (90, 150, 300, and 1200 discretizations) generated in the previous section for evaluation. To benchmark our model, we also generated uniform discretizations with the same discretizations. Then, for both discretization

methods, transition probability matrices were generated using Algorithm 2.

We find that the GreedyCut discretization method is able to better approximate the disease dynamics over the uniform discretization method. As shown in Figure 6, a comparison between the GreedyCut and the uniform discretization methods based on 300 discretizations shows that the Markovian trajectories for the GreedyCut discretization methods are closely aligned with the actual trajectories. However, the uniform discretization method shows poor approximation, especially showing incorrect trends for the proportion of the population infected over time – where the proportion of the population infected over time starts to decline after week 8 in the Markovian trajectory, whereas the proportion of infected people over time increases in the entire time horizon in the actual trajectory. Additionally, the uniform overestimates the proportion of recovered populations by more than twice compared with the actual proportion of infected people.

$ G $	GreedyCut		Uniform	
90	0.1411	[0.1264, 0.1558]	0.3269	[0.2388, 0.4150]
150	0.1300	[0.1162, 0.1439]	0.2483	[0.1887, 0.3708]
300	0.1218	[0.1087, 0.1350]	0.1969	[0.1729, 0.2210]
1200	0.1205	[0.1071, 0.1339]	0.1797	[0.1617, 0.1977]

Table 4.: Mean squared error for the trajectories given different numbers of discretizations

For all comparison pairs, the GreedyCut discretization method outperforms the uniform discretization method in the squared error between Markovian and actual trajectories. In Table 4, we show the result of the comparison of  $\mathbb{E}_{\hat{\theta} \in \hat{\Theta}} [\|\{\tilde{\mathbf{X}}_t\} - \{\mathbf{X}_t\}\|^2]$  over 1000 samples and 10 time periods between the GreedyCut and uniform discretization methods. Both algorithms are able to improve the result of approximation when the number of discretizations used increases, as expected. However, the improvement in approximations for the GreedyCut discretization method is small compared with uniform discretization, which suggests a high budget may not be necessary. When the number of allowable discretizations is small due to the computational budget, the GreedyCut discretization method can provide a much better approximation than the uniform discretization method, and adding discretizations may not add much accuracy.

## 5.2. Example 2: COVID-19

COVID-19 led to a significant surge in infections within Los Angeles County (LAC). To mitigate the pandemic during its initial phases, LAC implemented a lockdown from the second week to the tenth week following March 1st, 2020, which marked the onset of the epidemic. In this example, we use an MDP with discretizations to identify the optimal timing of imposing lockdowns in LAC to minimize the proportion of infected cases while considering the cost of a lockdown.

### 5.2.1. Model Structure and Inputs

To describe the disease dynamics of COVID-19 in LAC, we calibrated a SIR model that is stratified by health districts (HD) (Redelings, Lieb, & Sorvillo, 2010), meaning that the model allows for heterogeneity in health outcomes across HDs. The transmission rates between HDs is also allowed to vary. The disease dynamics for HD  $i$  are then

described as follows:

$$\begin{aligned}
S_{t+1}^i &= S_t^i - \sum_j \beta_{ji} S_t^i I_t^j \\
I_{t+1}^i &= I_t^i + \sum_j \beta_{ji} S_t^i I_t^j - \gamma I_t^i \\
R_{t+1}^i &= R_t^i + \gamma I_t^i
\end{aligned}$$

We use  $\beta_{ij}$  to represent the transmission rate from HD  $i$  to HD  $j$ , and all HDs are assumed to have the same clearance rate. We consider whether to implement a lockdown policy at each decision epoch,  $\Delta t$ , which has a duration of one week. Decisions need to be made over a total time horizon of 60 weeks ( $N=60$ ). If lockdown is implemented, transmission will be reduced ( $\beta$  decreases 80%).

We assume there were 1000 infections (0.01% of the total population) at the initial time epoch. This is consistent with the early stage of the COVID-19 epidemic in LAC where the proportion of the population infected remains a small proportion of the overall population. To calibrate the parameters of the stratified SIR model, we used empirical COVID-19 data of case counts to calibrate transmission rate  $\beta$  and recovery rate  $\gamma$  (City of Los Angeles Public Health, 2023). LAC mobility data is also used to help capture the heterogeneity in transmission rate among HDs (Caltrans, 2023; Yu, Zhang, Suen, Dessouky, & Ordonez, 2024).

We let the stage costs be the proportion of the population infected plus the dis-utility if lockdown is implemented. We assume that the dis-utility without a policy intervention is zero. However, determining the dis-utility associated with a lockdown is challenging. If the dis-utility is excessively low, the optimal choice consistently leans towards implementing the lockdown, which ignores the potential economic and social burden brought by the lockdown. On the contrary, if the dis-utility proves to be excessively burdensome, it will never be enforced. To better reflect this tradeoff, we assume the dis-utility of implementing a one-week lockdown is 0.005, implying it equates to the dis-utility of 0.5% of the population infected per epoch.

We create two discretized MDPs with 150 discretizations using the GreedyCut discretization method and compare outcomes against that of a uniform discretization method. This will guarantee the completion of model construction within an hour for both the GreedyCut and the uniform discretization methods.

### 5.2.2. MDP Results

We compared the optimal action recommended by the discretized state MDP from the GreedyCut and uniform discretization methods. We find that our GreedyCut algorithm outperforms the uniform discretization by identifying a better MDP optimal solution with a smaller cumulative proportion of the population infected. Figure 7 shows a comparison of disease dynamics across different policies. Compared with no lockdown, the empirical policy in LAC (lockdown from week 2 to week 10) does not prevent but rather postpones infections (the total cumulative proportion of the population infected over time is 0.7504 in the empirical policy, and 0.7508 if no intervention is used). Both uniform-discretized and GreedyCut discretized MDPs are able to reduce the cumulative proportion of infections and the peak of infections. Comparing the two MDP solutions, the GreedyCut discretization method outperforms the uniform discretization method in terms of the overall reduction in the proportion of the

population infected by 0.4793 over the 60-week time horizon.

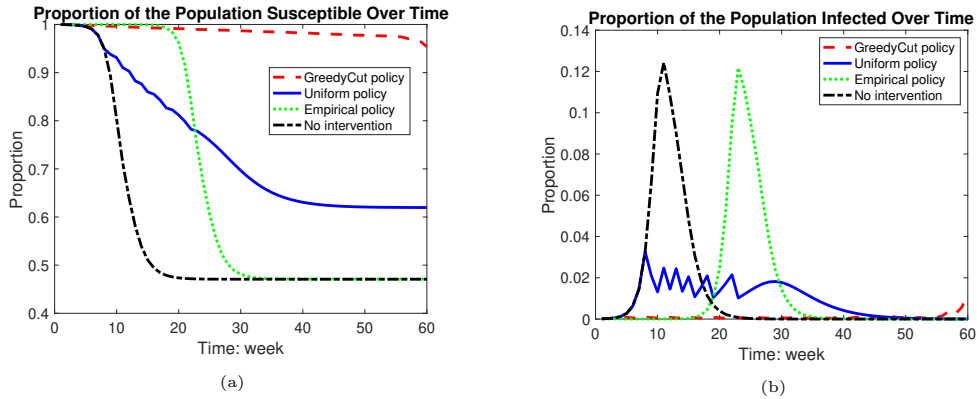


Figure 7.: Proportions of the population that is susceptible/infected over time.

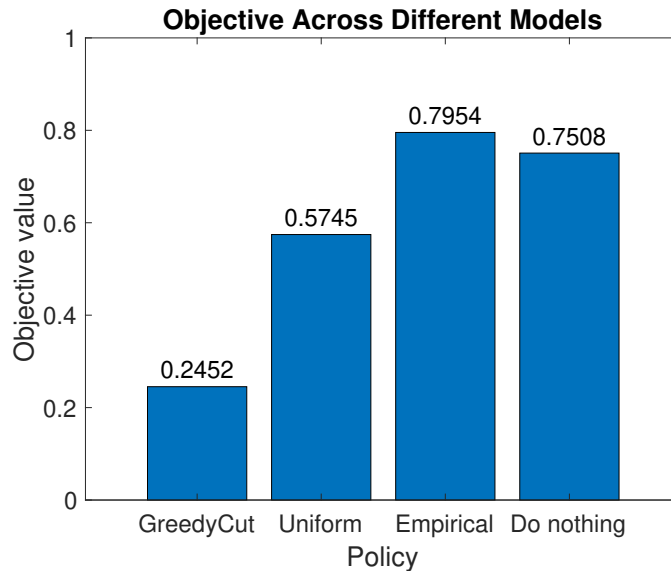


Figure 8.: Comparison between objective values across policies from GreedyCut MDP, uniform MDP, empirical policy, and no policy.

GreedyCut outperforms uniform, empirical, and ‘do nothing’ policies by achieving the lowest objective value (proportion of infected people over time plus lockdown disutility). Figure 8 compares the objective value among different models evaluated on the ground-truth disease (compartmental) model. The 8-week empirical lockdown policy LAC imposed has a lower objective value than doing nothing after considering the cost of lockdown, as it was not able to reduce infections while incurring lockdown disutility costs. Both uniform and GreedyCut MDPs provide a better solution. GreedyCut MDP is able to improve the objective value from doing nothing by 67% and outperforms the uniform MDP outcome by 57%.

This example demonstrates that the GreedyCut algorithm is able to provide a solution that has a smaller total cost compared to the empirical lockdown policy in LAC and the policy generated by the uniform discretized MDP. Even when the number of discretizations is limited for each compartment (for example, a stratified compartment-



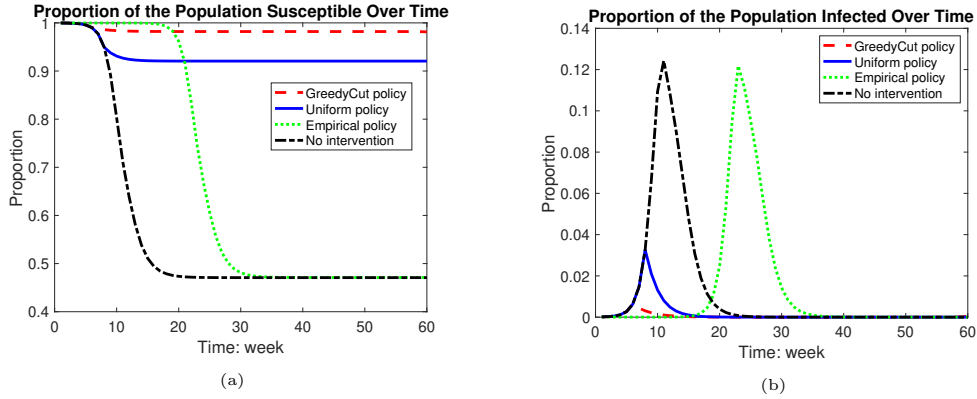


Figure 10.: Proportion of the population susceptible/infected over time for different MDPs with policy constraints.

MDP which could reduce the economic and societal burden brought by the lockdown.

## 6. Conclusions

In this paper, we introduce a novel algorithm for formulating an MDP framework tailored for continuous or large state-space problems in repeated decision-making with uncertainty for infected disease control. In our numerical analyses, we found that our algorithm provides better MDP solutions than the uniform discretized MDP for the models we evaluated. Our approach better approximates the true value function than the uniform discretized MDP, therefore leading to a better policy with a lower optimality gap. Compared to uniform discretization, our method demonstrates better performance across different discretization budgets, particularly showing notable benefits when the number of discretizations is small. This may be particularly pertinent for a compartmental model with many compartments, as the resultant number of discretizations for each compartment may be extremely limited. In this case, a uniform discretization method may result in a poor estimation of disease dynamics.

We found that our algorithm is able to provide a better state discretization than the uniform discretization method in approximating disease dynamics for the examples considered. Our approach generates smaller regions for states with a higher likelihood of being visited and increases the range of the region for those less frequently visited. Using the GreedyCut method would substantially improve the approximation quality, thus resulting in an improved decision-making process.

Additionally, we offer an effective method to compute the transition probability matrices for formulating MDPs given  $f(\mathbf{X}_t, \pi_t)$ , which may be a compartmental or simulation-based model. This helps us incorporate other common disease modeling frameworks into the MDP decision-making framework, facilitating the seamless integration of diverse healthcare applications. This approach is not only straightforward to implement but also effectively captures the complex function  $f(\mathbf{X}_t, \pi_t)$  that represents the dynamics of the disease in transition probability matrices.

With a small number of discretizations, the time spent discretizing the state using our approach is considerably smaller than the time required to produce transition probability matrices. In our examples, the time needed to formulate the discretized MDP using our approach is nearly equivalent to the time necessary for the construction

of a uniform discretized MDP. Therefore, our approach could offer an improvement to the MDP solution without substantially increasing computational expense under limited budgets.

We provide numeric examples to demonstrate the efficiency and effectiveness of our algorithm in discretizing continuous-state decision-making problems. Benchmarking the performance with the uniform discretization method, we demonstrate that our algorithm is able to generate preferable discretizations with a limited budget that is a good proxy of the ground truth system. We also demonstrate that our algorithm can generate better policies in both synthetic examples and a COVID-19 example. In the synthetic example, our algorithm outperforms the uniform discretization in all metrics for different discretization budgets. In the COVID-19 example, our algorithm improves the objective by nearly 100% from the uniform discretization.

Our numerical analysis also generated policy implications for social distancing policy during COVID-19 in LAC. The first policy implication is that the threshold of implementing the lockdown depends on the proportions of susceptible and infected (recommending implementing the lockdown if the proportions of infected and susceptible are above certain numbers). When the proportion of the population infected increases, the threshold of implementing the lockdown on the proportion of the susceptible population decreases. This is because a less susceptible population is needed to spread the disease as the infected population grows. Similarly, when the proportion of the susceptible population increases, the threshold of implementing the lockdown on the proportion of the infected population decreases. Secondly, a short lockdown interval may not effectively reduce the total number of cases, instead only delays the epidemic peak. To more effectively control cases, a prolonged lockdown period is needed.

We must acknowledge several limitations of this work. The GreedyCut algorithm may not find the discretization that globally minimizes the cost function. The performance gap between the GreedyCut and the uniform discretization methods is small with a large discretization budget. The GreedyCut algorithm may have computational difficulty if there is a large action space and does not consider continuous action spaces; this leaves an interesting optimization direction for future studies. The output of the GreedyCut algorithm may be sensitive to the choice of cost function; different choices may result in widely different discretization choices, thus requiring reevaluation of the objective function is changed.

Despite these limitations, we believe that this work provides an effective and easy-to-handle scheme for dealing with decision-making problems in large or continuous state spaces. Our paper provides insight into future work on improving the discretization of solving large-scale MDPs.

## Acknowledgements

Financial support for this study was provided in part by a National Science Foundation (grant no. 2237959).

## References

Ahn, J.-H., & Hornberger, J. C. (1996). Involving patients in the cadaveric kidney transplant allocation process: A decision-theoretic perspective. *Management Science*, 42(5), 629-641.



- Alagoz, O., Chhatwal, J., & Burnside, E. S. (2013). Optimal policies for reducing unnecessary follow-up mammography exams in breast cancer diagnosis. *Decision Analysis*, *10*(3), 200–224.
- Alagoz, O., Hsu, H. E., Schaefer, A. J., & Roberts, M. S. (2010). Markov decision processes: A tool for sequential decision making under uncertainty. *Medical Decision Making*, *30*, 474–483.
- Alagoz, O., Maillart, L. M., Schaefer, A. J., & Roberts, M. S. (2004). The optimal timing of living-donor liver transplantation. *Management Science*, *50*(10), 1420–1430.
- Alagoz, O., Maillart, L. M., Schaefer, A. J., & Roberts, M. S. (2007). Choosing among living-donor and cadaveric livers. *Management Science*, *53*(11), 1702–1715.
- Allen, L. J. (1994). Some discrete-time si, sir, and sis epidemic models. *Mathematical biosciences*, *124*(1), 83–105.
- Arruda, E. F., & do Val, J. B. R. (2008). Stability and optimality of a multi-product production and storage system under demand uncertainty. *European Journal of Operational Research*, *188*(2), 406–427.
- Arruda, E. F., Pereira, B. B., Thiers, C. A., & Tura, B. R. (2019). Optimal testing policies for diagnosing patients with intermediary probability of disease. *Artificial intelligence in medicine*, *97*, 89–97.
- Bäuerle, N., & Rieder, U. (2009). Mdp algorithms for portfolio optimization problems in pure jump markets. *Finance and Stochastics*, *13*(4), 591–611.
- Beckley, R., Weatherspoon, C., Alexander, M., Chandler, M., Johnson, A., & Bhatt, G. S. (2013). Modeling epidemics with differential equations. *Tennessee State University Internal Report*.
- Blanchard, J. D., Cermak, M., Hanle, D., & Jing, Y. (2014). Greedy algorithms for joint sparse recovery. *IEEE Transactions on Signal Processing*, *62*(7), 1694–1704.
- Blower, S., Koelle, K., & Mills, J. (2002). Health policy modeling: epidemic control, hiv vaccines, and risky behavior. *Quantitative evaluation of HIV prevention programs*, 260–289.
- Boucherie, R. J., & Van Dijk, N. M. (2017). *Markov decision processes in practice* (Vol. 248). Springer.
- Brauer, F. (2008). Compartmental models in epidemiology. *Mathematical epidemiology*, 19–79.
- Brooks, A., Makarenko, A., Williams, S., & Durrant-Whyte, H. (2006). Parametric pomdps for planning in continuous state spaces. *Robotics and Autonomous Systems*, *54*(11), 887–897.
- Caltrans. (2023). *Pems data source performance measurement system (pems) data source*. (Available at <https://dot.ca.gov/programs/traffic-operations/mpr/pems-source> (accessed October 30, 2023))
- Calvia, A., Gozzi, F., Lippi, F., & Zanco, G. (2023). A simple planning problem for COVID-19 lockdown: a dynamic programming approach. *Economic Theory*, 1–28.
- Capan, M., Ivy, J. S., Wilson, J. R., & Huddleston, J. M. (2017, June). A stochastic model of acute-care decisions based on patient and provider heterogeneity. *Health care management science*, *20*(2), 187–206.
- Carson, Y., & Maria, A. (1997). Simulation optimization: methods and applications. In *Proceedings of the 29th conference on winter simulation* (pp. 118–126).
- Chhatwal, J., Alagoz, O., & Burnside, E. S. (2010). Optimal breast biopsy decision-making based on mammographic features and demographic factors. *Operations Research*, *58*(6), 1577–1591.
- City of Los Angeles Public Health. (2023). *LA county COVID-19 data*. (Available at <http://publichealth.lacounty.gov/media/Coronavirus/data/> (accessed October 30, 2023))
- David, I., & Yechiali, U. (1985). A time-dependent stopping problem with application to live organ transplants. *Operations Research*, *33*(3), 491–504.
- Denton, B. T., Kurt, M., Shah, N. D., Bryant, S. C., & Smith, S. A. (2009). Optimizing the start time of statin therapy for patients with diabetes. *Medical Decision Making*, *29*(3),

- 351-367.
- Fu, Y., Jin, H., Xiang, H., & Wang, N. (2022). Optimal lockdown policy for vaccination during COVID-19 pandemic. *Finance research letters*, *45*, 102123.
- Giannoccaro, I., & Pontrandolfo, P. (2002). Inventory management in supply chains: a reinforcement learning approach. *International Journal of Production Economics*, *78*(2), 153–161.
- Goenka, A., Liu, L., & Nguyen, M.-H. (2014). Infectious diseases and economic growth. *Journal of Mathematical Economics*, *50*, 34–53.
- Grimm, V., Mengel, F., & Schmidt, M. (2021). Extensions of the seir model for the analysis of tailored social distancing and tracing approaches to cope with COVID-19. *Scientific Reports*, *11*(1), 1–16.
- Harko, T., Lobo, F. S., & Mak, M. (2014). Exact analytical solutions of the susceptible-infected-recovered (sir) epidemic model and of the sir model with equal death and birth rates. *Applied Mathematics and Computation*, *236*, 184–194.
- Hu, C., Lovejoy, W. S., & Shafer, S. L. (1996). Comparison of some suboptimal control policies in medical drug therapy. *Operations Research*, *44*(5), 696-709.
- Kai, D., Goldstein, G.-P., Morgunov, A., Nangalia, V., & Rotkirch, A. (2020). *Universal masking is urgent in the COVID-19 pandemic: Seir and agent based models, empirical validation, policy recommendations*.
- Kaplan, R. M., Anderson, J. P., et al. (1996). The general health policy model: an integrated approach. *Quality of life and pharmacoeconomics in clinical trials*, *2*, 302–322.
- Kermack, W., & McKendrick, A. (1991). Contributions to the mathematical theory of epidemics—iii. further studies of the problem of endemicity. *Bulletin of mathematical biology*, *53*(1-2), 89–118.
- Kermack, W. O., & McKendrick, A. G. (1991a). Contributions to the mathematical theory of epidemics—i. 1927. *Bulletin of mathematical biology*, *53*(1-2), 33–55.
- Kermack, W. O., & McKendrick, A. G. (1991b). Contributions to the mathematical theory of epidemics—ii. the problem of endemicity. *Bulletin of mathematical biology*, *53*(1-2), 57–87.
- Kopec, J. A., Finès, P., Manuel, D. G., Buckeridge, D. L., Flanagan, W. M., Oderkirk, J., ... others (2010). Validation of population-based disease simulation models: a review of concepts and methods. *BMC public health*, *10*, 1–13.
- Kreke, J. E. (2007, September). *Modeling disease management decisions for patients with pneumonia-related sepsis*.
- Kröger, M., & Schlickeiser, R. (2020). Analytical solution of the sir-model for the temporal evolution of epidemics. part a: time-independent reproduction factor. *Journal of Physics A: Mathematical and Theoretical*, *53*(50), 505601.
- Kurt, M., Denton, B. T., Schaefer, A. J., Shah, N. D., & Smith, S. A. (2011). The structure of optimal statin initiation policies for patients with type 2 diabetes. *IIE Transactions on Healthcare Systems Engineering*, *1*(1), 49-65.
- Lefèvre, C. (1981). Optimal control of a birth and death epidemic process. *Operations Research*, *29*(5), 971–982.
- Liu, S., Brandeau, M. L., & Goldhaber-Fiebert, J. D. (2017, Mar). Optimizing patient treatment decisions in an era of rapid technological advances: the case of hepatitis c treatment. *Health care management science*, *20*(1), 16-32.
- Long, E. F., Nohdurft, E., & Spinler, S. (2018). Spatial resource allocation for emerging epidemics: A comparison of greedy, myopic, and dynamic policies. *Manufacturing & Service Operations Management*, *20*(2), 181–198.
- Lovejoy, W. S. (1991). Computationally feasible bounds for partially observed markov decision processes. *Operations research*, *39*(1), 162–175.
- Magni, P., Quaglino, S., Marchetti, M., & Barosi, G. (2000). Deciding when to intervene: a markov decision process approach. *International Journal of Medical Informatics*, *60*(3), 237 - 253.
- Maillart, L. M., Ivy, J. S., Ransom, S., & Diehl, K. (2008). Assessing dynamic breast cancer screening policies. *Operations Research*, *56*(6), 1411-1427.

- Mason, J., Denton, B., Shah, N., & Smith, S. (2014). Optimizing the simultaneous management of blood pressure and cholesterol for type 2 diabetes patients. *European Journal of Operational Research*, 233(3), 727 - 738.
- Matrajt, L., Eaton, J., Leung, T., Dimitrov, D., Schiffer, J. T., Swan, D. A., & Janes, H. (2021). Optimizing vaccine allocation for COVID-19 vaccines shows the potential role of single-dose vaccination. *Nature communications*, 12(1), 3449.
- Mishalani, R. G., & Madanat, S. M. (2002). Computation of infrastructure transition probabilities using stochastic duration models. *Journal of Infrastructure systems*, 8(4), 139–148.
- Munos, R., & Moore, A. (2002). Variable resolution discretization in optimal control. *Machine Learning*, 49, 291–323.
- Pedrozo-Pupo, J. C., Pedrozo-Cortés, M. J., & Campo-Arias, A. (2020). Perceived stress associated with COVID-19 epidemic in colombia: an online survey. *Cadernos de saude publica*, 36, e00090520.
- Piguillem, F., & Shi, L. (2022). Optimal COVID-19 quarantine and testing policies. *The Economic Journal*, 132(647), 2534–2562.
- Pontryagin, L. S. (2018). *Mathematical theory of optimal processes*. Routledge.
- Puterman, M. L. (1994). *Markov decision processes: Discrete stochastic dynamic programming* (1st ed.). USA: John Wiley & Sons, Inc.
- Redelings, M., Lieb, L., & Sorvillo, F. (2010). Years off your life? the effects of homicide on life expectancy by neighborhood and race/ethnicity in los angeles county. *Journal of Urban Health*, 87, 670–676.
- Sandıkçı, B., Maillart, L. M., Schaefer, A. J., Alagoz, O., & Roberts, M. S. (2008). Estimating the patient’s price of privacy in liver transplantation. *Operations Research*, 56(6), 1393–1410.
- Sandıkçı, B., Maillart, L. M., Schaefer, A. J., & Roberts, M. S. (2013). Alleviating the patient’s price of privacy through a partially observable waiting list. *Management Science*, 59(8), 1836–1854.
- Schaefer, A. J., Bailey, M. D., Shechter, S. M., & Roberts, M. S. (2004). Modeling medical treatment using markov decision processes. In M. L. Brandeau, F. Sainfort, & W. P. Pierskalla (Eds.), *Operations research and health care: A handbook of methods and applications* (pp. 593–612). Boston, MA: Springer US.
- Shechter, S. M., Bailey, M. D., Schaefer, A. J., & Roberts, M. S. (2008). The optimal time to initiate hiv therapy under ordered health states. *Operations Research*, 56(1), 20–33.
- Singh, R., Liu, F., & Shroff, N. B. (2020). A partially observable mdp approach for sequential testing for infectious diseases such as COVID-19. *arXiv preprint arXiv:2007.13023*.
- Sonnenberg, F. A., & Beck, J. R. (1993). Markov models in medical decision making: A practical guide. *Medical Decision Making*, 13(4), 322–338.
- Suen, S.-c., Bendavid, E., & Goldhaber-Fiebert, J. D. (2014). Disease control implications of india’s changing multi-drug resistant tuberculosis epidemic. *PloS one*, 9(3), e89822.
- Suen, S.-c., Brandeau, M., & Goldhaber-Fiebert, J. G. (2018). Optimal timing of drug sensitivity testing for patients on first-line tuberculosis treatment. *Health Care Management Science*, 21, 632–646.
- Talbot, T. R., Bradley, S. F., Cosgrove, S. E., Ruef, C., Siegel, J. D., & Weber, D. J. (2005). Influenza vaccination of healthcare workers and vaccine allocation for healthcare workers during vaccine shortages. *Infection Control & Hospital Epidemiology*, 26(11), 882–890.
- Topkis, D. M. (2011). *Supermodularity and complementarity*. Princeton university press.
- Tuite, A. R., Burchell, A. N., & Fisman, D. N. (2014). Cost-effectiveness of enhanced syphilis screening among hiv-positive men who have sex with men: a microsimulation model. *PloS one*, 9(7), e101240.
- Webster, R. K., Brooks, S. K., Smith, L. E., Woodland, L., Wessely, S., & Rubin, G. J. (2020). How to improve adherence with quarantine: rapid review of the evidence. *Public health*, 182, 163–169.
- Wu, C., Luo, C., Xiong, N., Zhang, W., & Kim, T.-H. (2018). A greedy deep learning method for medical disease analysis. *IEEE Access*, 6, 20021–20030.

- Yaesoubi, R., & Cohen, T. (2011). Generalized markov models of infectious disease spread: A novel framework for developing dynamic health policies. *European journal of operational research*, 215(3), 679–687.
- Yu, H., Zhang, S., Suen, S.-c., Dessouky, M., & Ordonez, F. (2024). Extending dynamic origin-destination estimation to understand traffic patterns during COVID-19. *arXiv preprint arXiv:2401.10308*.
- Zhang, F., Wagner, A. K., & Ross-Degnan, D. (2011). Simulation-based power calculation for designing interrupted time series analyses of health policy interventions. *Journal of clinical epidemiology*, 64(11), 1252–1261.
- Zhang, S., Suen, S.-C., Gong, C. L., Pham, J., Trebicka, J., Duvoux, C., ... Sundaram, V. (2021). Early transplantation maximizes survival in severe acute-on-chronic liver failure: results of a markov decision process model. *JHEP Reports*, 3(6), 100367.
- Zhao, Z., Zhou, M., & Liu, S. (2021). Iterated greedy algorithms for flow-shop scheduling problems: A tutorial. *IEEE Transactions on Automation Science and Engineering*.
- Zhou, E., Fu, M. C., & Marcus, S. I. (2010). Solving continuous-state pomdps via density projection. *IEEE Transactions on Automatic Control*, 55(5), 1101–1116.

This figure "COVID\_obj\_switch.jpg" is available in "jpg" format from:

<http://arxiv.org/ps/2404.12540v1>

This figure "runtime.jpg" is available in "jpg" format from:

<http://arxiv.org/ps/2404.12540v1>